Research Article

EXPERIMENTAL AND NUMERICAL INVESTIGATION OF THE EFFECTS OF VORTEX FINDER GEOMETRY ON CYCLONE PERFORMANCE

Aykut KARADENİZ*[1], Coşkun AYVAZ[2], Selami DEMİR[3], Murat AKSEL[4], Arslan SARAL[5]

[1]*Dept. of Environmental Eng., Yıldız Technical University, ISTANBUL;* ORCID: 0000-0002-9754-9088
[2]*Istanbul University Cerrahpaşa, Dept. of Environmental Eng.,ISTANBUL;* ORCID: 0000-0003-0052-0842
[3]*Dept. of Environmental Eng., Yıldız Technical University, ISTANBUL;* ORCID: 0000-0002-8672-9817
[4]*Alanya Alaaddin Keykubat University, Department of Civil Engineering, ANTALYA;*
ORCID: 0000-0002-6456-4396
[5]*Dept. of Environmental Eng., Yıldız Technical University, ISTANBUL;* ORCID: 0000-0001-5684-5449

ABSTRACT

In this study, nine different vortex finders (VFs) were used for investigations on cyclone pressure drop and particle collection efficiency. The collection efficiencies dropped for larger and smaller vortex finder dimension (VFDs). The collection efficiency increased with increasing vortex finder lengths (VFL). This increase was more obvious and statistically meaningful for the smallest VFD. Pressure drop in cyclones were mainly a function of VFD and increased with decreasing VFD. These effects were also observed in Computational Fluid Dynamics (CFD) simulations. A performance map was built for the design of a VF optimized for the highest collection efficiency and the lowest pressure drop.
Based on the experimental results, a mathematical model was developed, and the nickel inhibition constants (KNi) were found to be 8.75 mg/L.
Keywords: Cyclones, vortex finder, pressure drop, collection efficiency, computational fluid dynamics.

---

1. INTRODUCTION

Cyclone separators are simple devices in which flue gas containing particulate matter is forced into a spinning motion that results in a centrifugal force [1]. As a result of the spinning motion of the flue gas within the cyclone separator, particles, being heavier than the gaseous components, drift toward and collide with the outer wall of the cyclone, and moves along the flue gas-cyclone wall boundary. A conical part that is attached to the lower part of the cyclone body is employed to divert the gaseous flow toward the vortex finder while particles cannot be diverted and they fall into a dust bin attached to the conical part, leaving the cleaned gas stream at the exit of the separator.

Cyclone separators are mainly used both to meet particulate emission limits and to reduce particulate loading into subsequent control devices. They offer advantages such as simple construction, and low operation and maintenance costs. Besides, cyclone separators can adapt

---

* Corresponding Author: e-mail: aykutk@yildiz.edu.tr, tel: (212) 383 54 06

extreme operating conditions such as high temperature, high pressures, and high particle loads [2, 3].

Pressure drop and collection efficiency are the two parameters that defines the performance of a given cyclone. These parameters are intimately related with each other and the collection efficiency usually increases with increased pressure drop up to some certain level, above which re-entrainment of particles reduce the collection efficiency. Of these, pressure drop is mainly a function of cyclone geo metry and a great number of research papers have been dedicated to improving the cyclone geometry to reduce pressure drop while increasing the collection efficiency [1, 4-12]. On the other hand, Computational Fluid Dynamics (CFD) models are also used for cyclone separators to predict flow pattern and estimate pressure drop as well as particle collection efficiency [2, 3, 13-20]. Although not as efficient for practical use as for scientific use, CFD simulations help scientists develop cyclone dimensions improved for better performance. Of these dimensions, the vortex finder (VF) is of considerable importance since the diameter (VFD) and the length (VFL) of the vortex finder have a clear impact on the behavior of the inner and outer vortices within the cyclone separator. Saltzman and Hochstrasser [21] used a number of different VFDs to examine their effects on cyclone performance. Moore and Mcfarland [22] stated that VFD affects the cut diameter, while Kim and Lee [23] also studied the effects of VFD on particle collection efficiency. On the other hand, Zhu and Lee [24] studied the effects of VFL on particle collection efficiency, reporting that increasing the VFL up to a certain value results in increased particle collection efficiency. In another research, Lim et al [15] reported that the collection efficiency varies with the shape of the vortex finder.

The aim of this study is to investigate experimentally the effects of VFL and VFD on particle collection efficiency and pressure drop. The paper presents the experimental pressure drop and overall collection efficiency. Besides, CFD simulations are performed to estimate the effects of VF on the flow and pressure fields within the cyclones in order to make better conclusions on how the collection efficiency is affected by VFD and VFL.

2. MATERIALS AND METHODS

2.1. Experimental Setup

The laboratory-scale experimental setup was composed of a high-pressure fan, a dust generator, and the cyclone separator. A schematic representation of the setup is shown in Fig. 1. The fan was located downstream of the cyclone separator and the system was operated in vacuum mode. The capacity of the fan was 1500 m³/h and the flowrate through the cyclone was measured by a digital differential pressure transmitter installed at the downstream of the fan. The capacity of the dust generator was 10 kg/h. The cyclone separators used were of Stairmand-high-efficiency type except the VF dimensions. Table 1 summarizes the cyclone geometries.
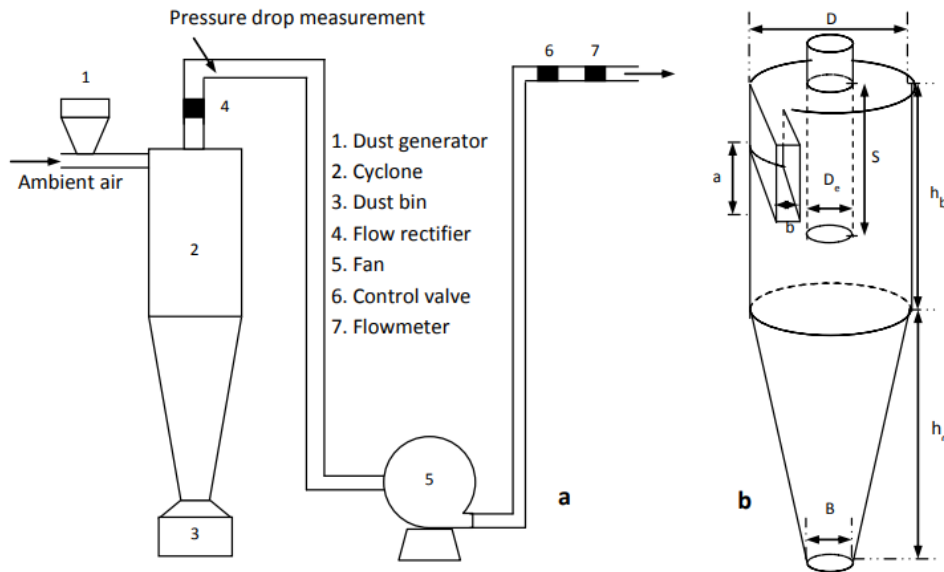
Figure 1. Schematic rep resentation of **a.** the experimental setup, and **b.** cyclone dimensions

Table 1. Dimensions of cyclones used

Cyclone geometry	Notation	Dimension (mm)	Ratio	Remarks*
Body diameter	D	290	–	Constant for all runs.
Inlet height	a	145	0.50	Constant for all runs.
Inlet width	b	58	0.20	Constant for all runs.
Body height	h_b	435	1.50	Constant for all runs.
Conical height	h_c	725	2.50	Constant for all runs.
Vortex finder length (VFL)	S_1	145	0.50	Limitations in construction forced combined design of these two parameters. A total of nine VFs were used.
	S_2	174	0.60	
	S_3	203	0.70	
Vortex finder diameter (VFD)	D_{e1}	116	0.40	
	D_{e2}	145	0.50	
	D_{e3}	174	0.60	
Cone-tip diameter	B	109	0.38	Constant for all runs.
Purpose of experimental use. Various combinations of two parameters (vortex finder length and diameter) offer nine different cyclone designs				

The diameter of the cyclones was 290 mm. A total of nine tangential-inlet cyclones were used (three distinct sizes for each of VFD and VFL). Flow rectifiers were used at the cyclone exit to straighten the streamlines for reliable pressure drop measurements. Pressure drop through the cyclone separators are expressed as the difference of static pressures at the cyclone inlet and the exit. Overall particle collection efficiencies of the cyclones were calculated as the ratio of the mass of particles collected in the dust bin to the mass of particles dosed during the experiment. Size distribution of particles was monitored by a Malvern Mastersizer Hydro2000MU.

2.2. CFD Simulations

To investigate the effects of geometrical changes, CFD analysis has been performed by FLUENT, which is a part of ANSYS Workbench Products. 3D solid model was designed in a CAD based program and meshed using over 1 million elements by using ANSYS Meshing Module. Inflation layers are created to minimize wall effects on flow domain (Fig. 2).
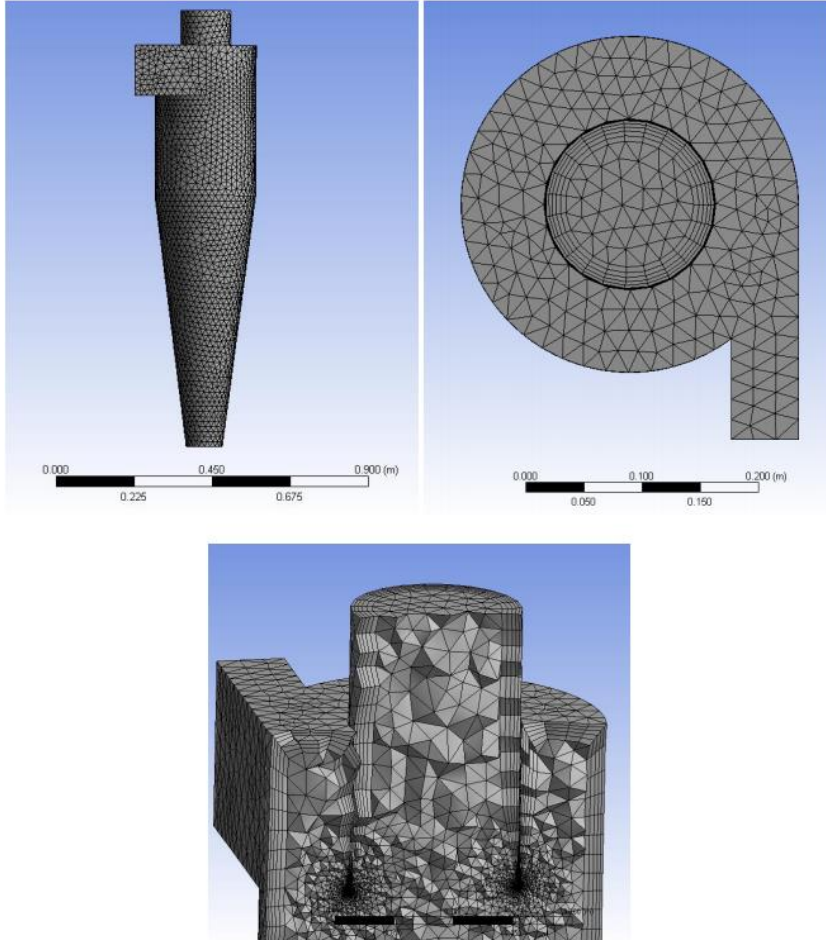

Figure 2. Meshed geometry and inflation layers

Pressure outlet boundary condition was defined at the outlet of the cyclone. At the inlet, velocity boundary was defined. Cyclone walls and dust bin were labeled as stationary wall boundaries. Solver parameters for ANSYS-Fluent are given in Table 2.

Table 2. Fluent analysis parameters

Analysis options	Properties
Solver type	Pressure based
Time	Steady
Turbulence model	Viscous
	RNG k-ε
	Standard wall function
Solution method	PISO
	Skewness correction: 1
	Neighbor correction:1
Spatial discretization	Gradient: Least squares cell based
	Pressure: Presto!
	Momentum: First order upwind
	Volume fraction: Geo-reconstruct
	Turbulent kinetic energy: First order upwind
Transient formulation	First order implicit

3. RESULTS AND DISCUSSIONS

The experimental setup was operated with ambient air into which fly ash particles from the electrostatic precipitator unit of a small power plant in a steel factory was dosed. The size distribution of particles is given in Fig. 3. Median diameter of fly ash particles were determined to be around 33 μm.
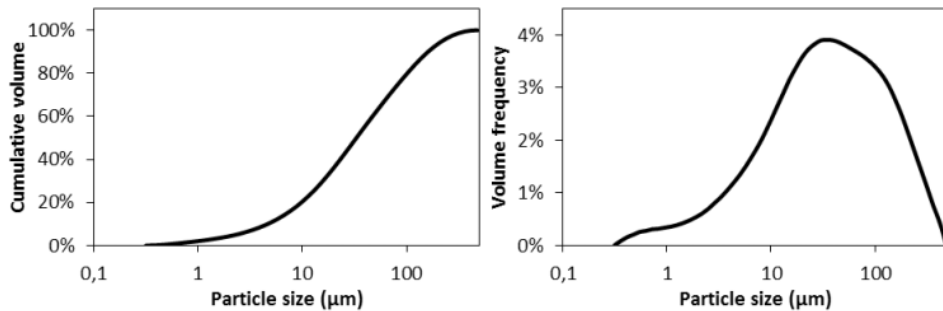

Figure 3. Size distribution of fly ash particles

The experimental setup was operated at a particle concentration of around 8 g/m³ . Five runs were performed for each VF geometry; and for each run, the dust generator was started after adjusting the flowrate to the desired value of around 562 m³/h, giving an inlet velocity of 18.5 m/s. The system was allowed to run for 10 minutes after the dust generator starts.

3.1. Experimental Results

The effects of VF dimensions (S and D_e) on pressure drop (ΔP) and particle collection efficiency (η) were investigated for nine distinct VFs with VFDs of $0.4D$, $0.5D$, and $0.6D$ and VFLs of $0.5D$, $0.6D$, and $0.7D$. Collection efficiencies are shown in Table 3.

Table 3. Particle collection efficiencies for distinct VF dimensions

Vortex finder diameters	Vortex finder lengths		
	0.5D	**0.6D**	**0.7D**
0.4D	97.8%±0.16	98.6%±0.22	98.1%±0.26
0.5D	95.8%±0.16	96.5%±0.32	96.4%±0.33
0.6D	94.3%±0.20	94.9%±0.34	94.8%±0.44
Uncertainties are given as standard deviations based on five runs			

The results show that geometry of the VF has a clear impact on particle collection efficiency. In order to check if differences in collection efficiencies are statistically meaningful, a t-test was performed to assess differences of average collection efficiencies. The discrepancies for varying VFDs and VFLs are shown in Table 4.

Table 4. Discrepancies between average collection efficiencies for various vortex finder geometries

Vortex finder lengths	Vortex finder lengths			Vortex finder diameters			Vortex finder diameters
	$S=0.5D$	$S=0.6D$	$S=0.7D$	$D_e=0.4D$	$D_e=0.5D$	$D_e=0.6D$	
	for $D_e = 0.4D$			for $S = 0.5D$			
$S=0.5D$	–	0.8±0.28	0.3±0.32	–	-2.0±0.23	3.5±0.26	$D_e=0.5D$
$S=0.6D$	-0.8±0.28	–	-0.5±0.36	2.0±0.23	–	-1.5±0.26	$D_e=0.6D$
$S=0.7D$	-0.3±0.32	0.5±0.36	–	3.5±0.26	1.5±0.26	–	$D_e=0.7D$
	for $D_e = 0.5D$			for $S = 0.6D$			
$S=0.5D$	–	0.7±0.36	0.6±0.38	–	-2.1±0.40	-3.7±0.42	$D_e=0.5D$
$S=0.6D$	-0.7±0.36	–	-0.1±0.47	2.1±0.40	–	-1.6±0.47	$D_e=0.6D$
$S=0.7D$	-0.6±0.38	0.1±0.47	–	3.7±0.42	1.6±0.47	–	$D_e=0.7D$
	for $D_e = 0.6D$			for $S = 0.7D$			
$S=0.5D$	–	0.6±0.40	0.5±0.50	–	-1.7±0.44	-3.3±0.53	$D_e=0.5D$
$S=0.6D$	-0.6±0.40	–	-0.1±0.57	1.7±0.44	–	-1.6±0.56	$D_e=0.6D$
$S=0.7D$	-0.5±0.50	0.1±0.57	–	3.3±0.53	1.6±0.56	–	$D_e=0.7D$

Values are based on five measurements for each VF geometry at 95% confidence level
Values are given as percent

For the shortest VFL (S= 0.5D), the collection efficiency decreased clearly with increasing VFD. The percent discrepancy between collection efficiencies of cyclones with VFDs of 0.4D and 0.6D was as high as 3.5%±0.26. For the other VFLs (S= 0.6D and S= 0.7D), the percent discrepancies between the collection efficiencies showed similar trends with increasing VFDs (right part of Table 4). For all VFLs, increasing the VFD in the range of 0.4D and 0.6D resulted in a clear decrease in collection efficiency. The collection efficiencies decreased by 3.3% to 3.7% on average by increasing the VFD for all VFLs.

For all VFDs, the collection efficiency showed slight increases when the VFL was increased from 0.5D to 0.6D. The percent changes were between 0.6% and 0.8% (left part of Table 4). The changes in collection efficiency were smaller when the VFL was increased from 0.5D to 0.7D, and the changes were calculated as 0.3%±0.32, 0.6%±0.38, and 0.5%±0.50, respectively for VFDs of 0.4D, 0.5D, and 0.6D. The decrease in collection efficiency by increasing VFL from 0.6D to 0.7D was negligible especially for VFDs of 0.5D and 0.6D (the interval calculated for collection efficiencies at 95% confidence includes zero for these VFDs). On the other hand, a meaningful decrease in collection efficiency was observed for VFD of 0.4D (0.5%±0.36).

Obviously, the highest collection efficiency was obtained for VFD and VFL of 0.4*D* and 0.6*D*, respectively. In order to check the sensitivity of collection efficiency, the changes in collection efficiency with respect to the change in VFD ($D \frac{\partial \eta}{\partial D_e}$) dimension were also calculated. The sensitivities ($D \frac{\partial \eta}{\partial D_e}$) were calculated as -2.0% and -1.5% per unit change in VFD (increasing VFD by 0.1*D*) for the VFL of 0.5*D*, as -2.1% and -1.6% for the VFL of 0.6*D*, and as -1.7% and -1.6% for the VFL of 0.7*D*. Obviously, the sharpest decrease in collection efficiency with respect to VFD was observed for the VFL of 0.6*D*, while the mildest decrease was observed for the VFL of 0.7*D*. The results showed that the collection efficiency is highly sensitive to the changes in VFD for the VFL of 0.6*D*. If the VFL is increased to 0.7*D*, on the other hand, the effect of changing VFD on the collection efficiency is smaller. Clearly, the best vortex finder dimensions for the highest collection efficiency are VFD = 0.4*D* and VFL = 0.6*D*, although the collection efficiency is highly sensitive to VFD for these dimensions. Also, one should note that these dimensions result in the highest collection efficiency and performance evaluations must include the pressure drop measurements.

Since the performance of a cyclone is basically defined by its particle collection efficiency and pressure drop, pressure drops were also measured to ensure a healthy optimization of VF geometry. Results for distinct VF dimensions are given in Table 5. Values in Table 5 are reported as clean pressure drop. Since the pressure drop decreases with increasing solids load [25], clean pressure drop represents maximum pressure drop during the cyclone operation and should be used for cyclone design and fan selection, etc. [26]. Formulations for estimating the decrease in pressure drop in cyclones operated at high solids load can be found in [27, 29].

Table 5. Pressure drop in the cyclones

Vortex finder diameter	Vortex finder length		
	0.5*D*	0.6*D*	0.7*D*
0.4D	1500	1649	1750
0.5D	766	791	800
0.6D	370	373	375
Values are given as pressure drop in N/m²			

The pressure drops changed between 370 and 1750 Pa for nine different vortex finders. The pressure drop was mainly a function of VFD, and increased with decreasing VFD. On the other hand, the pressure drop slightly increased with increasing VFL. The lowest pressure drop was observed for VFD = 0.6*D* and VFL = 0.5*D*, while the highest pressure drop was observed for VFD = 0.4*D* and VFL = 0.7*D*.

An optimum design may be developed in light of the experimental data for obtaining the highest collection efficiency at the lowest pressure drop. For this purpose, a performance map is prepared to determine the most cost-effective VF geometry and is given in Fig. 4. In figure, the color-scale represents clean pressure drop while isopleths show the particle collection efficiency. Using this map, one can easily decide vortex finder geometry with the lowest operational cost and the highest collection efficiency. For instance, selecting a set of VFD and VFL as 0.5*D* and 0.5*D*, respectively, results in an average collection efficiency of 95.8% at a pressure drop of 766 Pa. On the other hand, one can choose a set of VFD and VFL as 0.534*D* and 0.6*D*, respectively, to obtain the same particle collection efficiency at a pressure drop of around 604 Pa. This way, the designer reduces the pressure drop by around 27% without a significant change in particle collection efficiency. Similarly, a set of VFD and VFL as 0.4*D* and 0.535*D*, respectively, would yield the same average particle collection efficiency of around 98% with a set of VFD and VFL as 0.428*D* and 0.6*D*. The pressure drop in the former cyclone is around 1510 Pa while that in the latter one is 1420 Pa, which reduces the pressure drop by around 6%. Considering the fact that construction

costs are one-time costs at the investment stage, and operating costs are continuous, reduction of pressure drop by selecting different vortex finder geometry could lead to great savings in the operation stage.
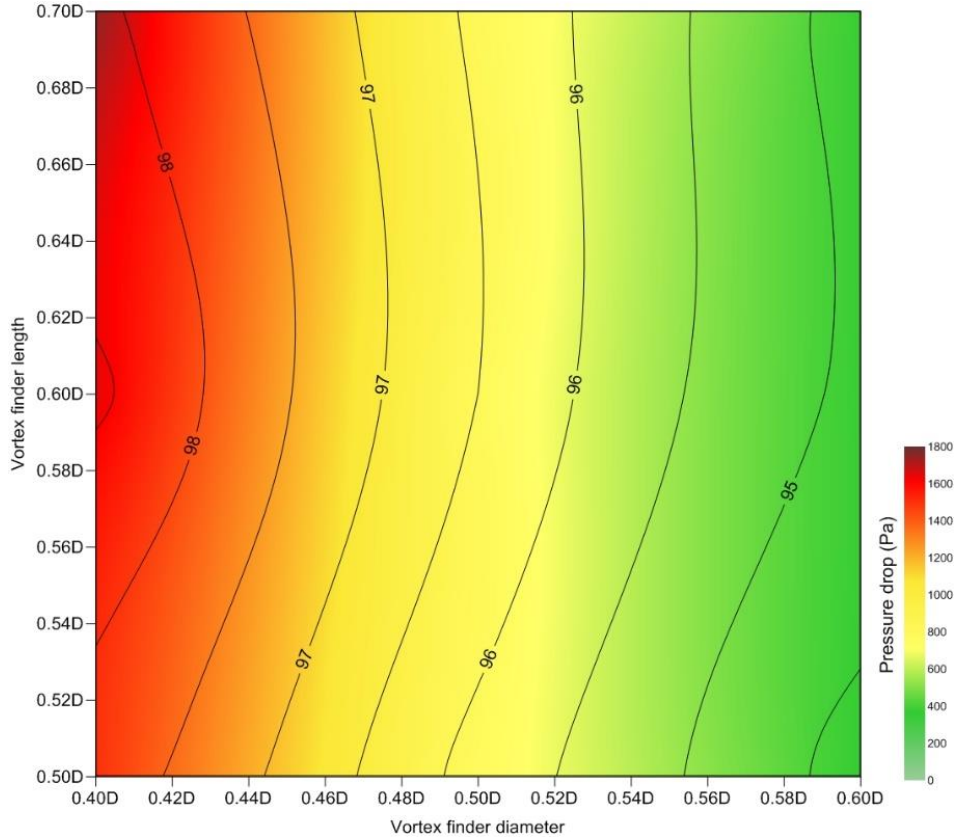

Figure 4. Cyclone collection efficiencies and pressure drops

3.2. CFD Results

Computational Fluid Dynamics analyses were also performed to simulate experimental conditions. Fig. 5 shows pressure fields in nine cyclones with VFDs ranging from $0.4D$ to $0.6D$ and VFLs in the range of $0.5D$ to $0.7D$.

For all cyclones, the static pressure shows a decreasing trend in radial direction from wall toward the center. The highest pressure gradients were observed at the vortex finder entrance, where negative pressures were observed for all cyclones. In contrast, the pressure gradient was negligible in axial direction, showing that the pressure drop due to friction within the cyclone body was minimal and most of pressure drop took place at the inlet and vortex finder. Fig. 5 clearly shows that the flow was not symmetrical. The symmetry of flow was poorer as the VFD increases from $0.5D$ to $0.6D$. The central region of the swirl was the most twisted for VFD = $0.6D$ and VFL = $0.7D$.

The diameter of the vortex finder, being in the expansion zone at the inlet side, also affected the outer vortex. This effect is obvious both in Fig. 5 and Fig. 6, which shows tangent velocity

profile within cyclones. At the inlet side, increasing VFD caused decreased cross-sectional area leading to increased tangent velocity in this zone.
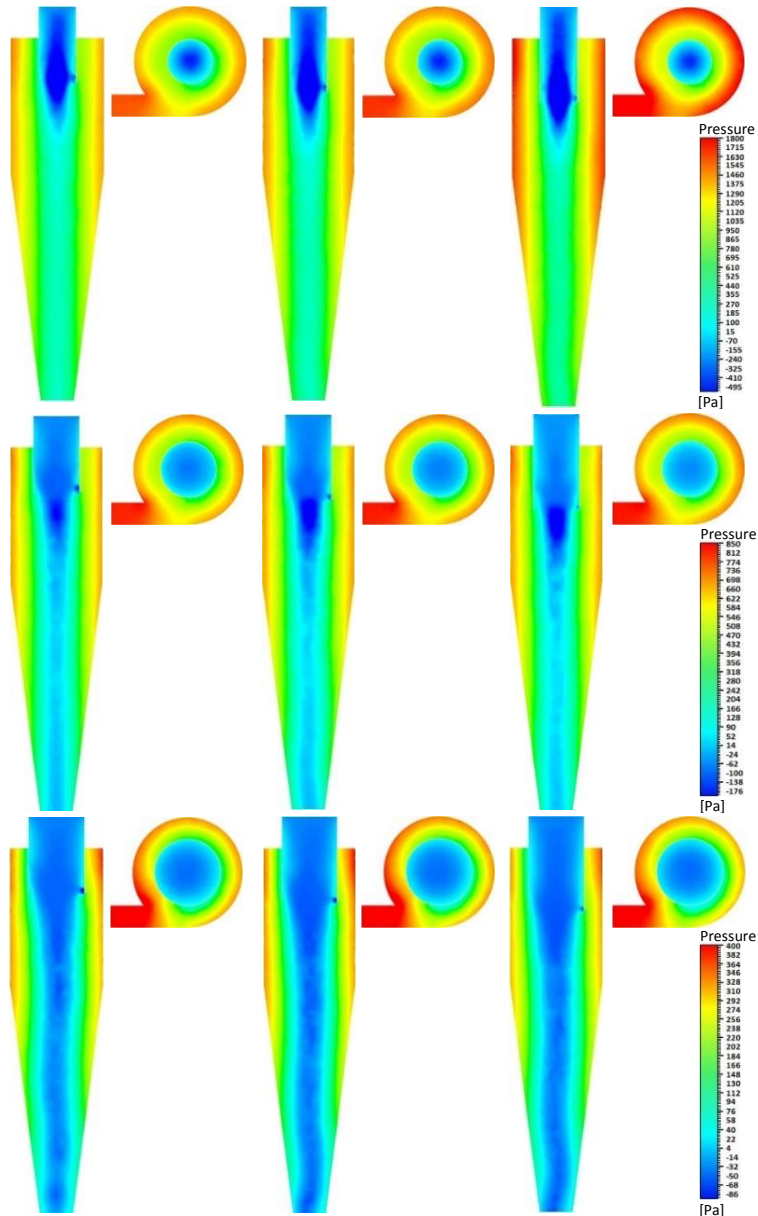

Figure 5. Pressure fields in cyclones. VFLs 0.5*D*, 0.6*D*, and 0.7*D* (from left to right). VFDs 0.4*D*, 0.5*D*, and 0.6*D* (from top to bottom)
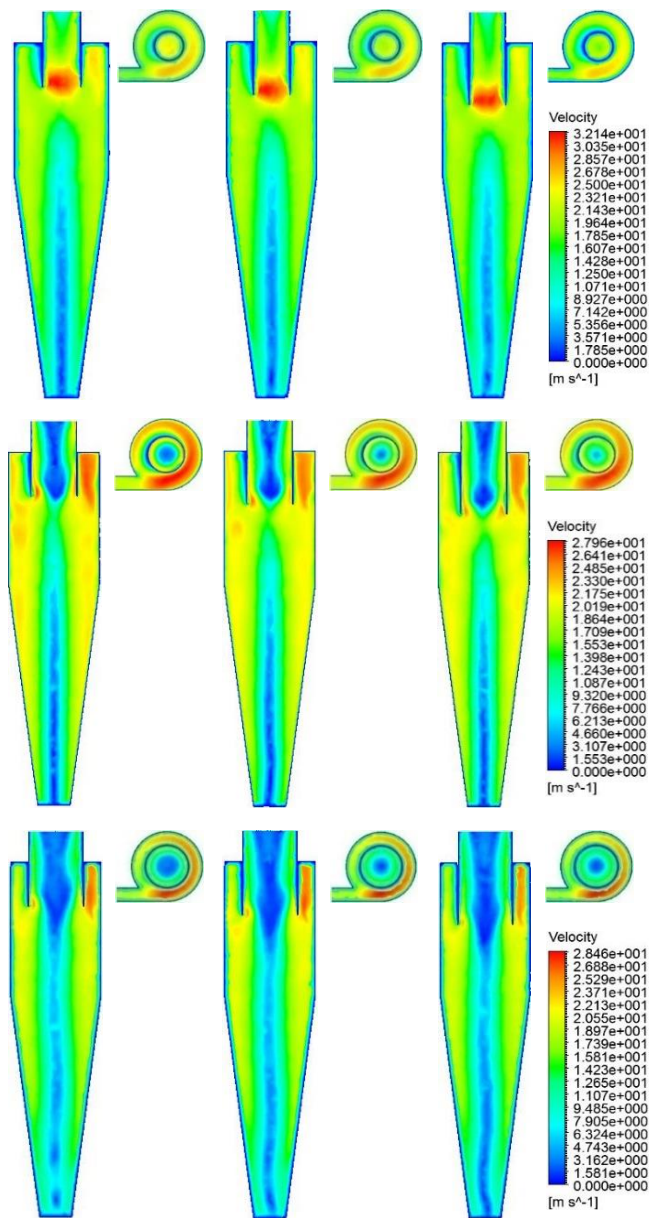
Figure 6. Tangent velocity profiles in cyclones. VFLs 0.5*D*, 0.6*D*, and 0.7*D* (from left to right). VFDs 0.4*D*, 0.5*D*, and 0.6*D* (from top to bottom)

Fig. 6 indicates that the tangential velocity increased with radius toward the wall till the outer boundary of the inner vortex, where it reached a radial maximum and started to decrease with increasing radial distance to the center. At the wall, tangential velocity becomes zero. This behavior of the swirling flow is called a Rankine vortex with forced vortex in the inner region and

free vortex at the outer region. For Rankine type vortices, the tangent velocity distribution along the radial distance for a given section can be estimated easily. Fig. 6 also shows that the tangential velocity could be as high as 1.75 times the average inlet velocity within the cyclone. Tangential velocity was the highest at the entrance of vortex finder for VFD = 0.4*D*. On the other hand, the highest tangential velocity for VFD = 0.5*D* and VFD = 0.6*D* was observed in the outer vortex at the middle of inlet height, where swirling flow forms.

In Fig. 5 and Fig. 6, it is obvious that VFD has a clear effect on static pressure and tangent velocity profiles. This effect is obvious for especially VFD = 0.6*D*. Increasing VFD disturbs the inner vortex, which is considered as the reason for reduced collection efficiency in cyclones with VFD = 0.6*D*.

4. CONCLUSIONS

An experimental setup was built to investigate the effects of vortex finder (VF) dimensions on cyclone performance. For this purpose, nine VFs with three different VFDs (0.4*D*, 0.5*D*, and 0.6*D*) and three different VFLs (0.5*D*, 0.6*D*, and 0.7*D*) were used. All other dimensions were of Stairmand high efficiency type cyclone. The body diameter of the cyclones was 290 mm. Experiments were performed at 562 m³/h ambient air with an inlet velocity of 18.5 m/s. Fly ash particles were used for experiments. Overall particle collection efficiencies and clean pressure drops were measured experimentally. Overall particle collection efficiencies ranged from 94.3%±0.22% to 98.6%±0.20%. The pressure drop in the cyclones with these particle collection efficiencies were 370 and 1649 N/m² , respectively. On the other hand, the highest pressure drop was measured in the cyclone with VFL = 0.7*D* and VFD = 0.4*D* as 1750 N/m² . The overall particle collection efficiency for this cyclone was 98.1%±0.26%. CFD simulations were also performed for the experimental cyclones. Finally, a performance map was prepared for selecting the most economical design for vortex finder.

Following conclusions can be withdrawn based on the results of this study:

- VF design has a clear impact on both pressure drop and particle collection efficiency. Thus, VF dimensions should be carefully chosen in the design.

- Collection efficiency increases with increasing VFL up to a certain point above which increasing VFL further leads to reduced collection efficiencies. Pressure drop also increases with increasing VFL by around 0.5% to 9% for all VFDs.

- Negligible pressure gradient in axial direction shows that pressure drop due to friction within the cyclone body is minimal and most of the pressure drop takes place at the inlet and vortex finder.

- In order to design an optimized VF, the pressure drop and collection efficiency must be considered together. A performance map is presented which allows selection of dimensions of a VF optimized in the aspect of pressure drop and particle collection efficiency.

- One should note that the collection efficiencies were obtained with the fly ash particles used in this study. The collection efficiencies may vary with particles' properties and the designer should take this into account during the design process especially if the cyclone separator is the main collection device. Besides, the performance map provided in this study is valid for VFDs between 0.4*D* and 0.6*D*, and VFLs between 0.5*D* and 0.7*D*.

- According to the conditions in this study, 75% savings in pressure drop can be achieved against only a 4% reduction in particle collection efficiency. This is a positive result for overall cyclone performance.

- Finally, as it is clear from the results, the VFD is more important than VFL on cyclone performance.

Acknowledgement

REFERENCES

[1]   Ioza, D.L. and Leith, D. (1989) Effect of cyclone dimensions on gas flow pattern and collection efficiency. *Aerosol Science and Technology*, 10, 491-500.

[2]   Elsayed, K. and Lacor, C. (2010) The effect of vortex finder diameter on cyclone separator performance and flow field. *5th European Conference on Computational Fluid Dynamics*, Lisbon, Portugal.

[3]   Elsayed, K. and Lacor, C. (2011) Numerical modeling of the flow field and performance in cyclones of different cone-tip diameters, *Computers & Fluids*, 51, 44-59.

[4]   Stairmand, C.J. (1951) The design and performance of cyclone separators, *Transaction of the. Institution of Chemical Engineers*, 29, 356-383.

[5]   Lapple, C.E. (1951) Processes use many collector types, *Chemical Engineering*, 58, 144-151.

[6]   Hoffmann, A.C., van Santen, A. and Allen, R.W.K. (1992) Effects of geometry and solid loading on the performance of gas cyclones, *Powder Technology*, 70, 83-91.

[7]   Yetilmezsoy, K. (2005) Optimization using prediction models: Air cyclones' body diameter/pressure drop, *Filtration & Seperation*, 42(10), 32-35.

[8]   Brar, L.S., Sharma, R.P. and Elsayed, K. (2015) The effect of the cyclone length on the performance of Stairmand high-efficiency cyclone, *Powder Technology*, 286, 668-677.

[9]   Demir, S., Karadeniz, A. and Aksel, M. (2016) Effects of cylindrical and conical heights on pressure and velocity fields in cyclones, *Powder Technology*, 295, 209-217.

[10]   Misiulia, D., Andersson, A.G. and Lundström, T.S. (2017) Effects of the inlet angle on the collection efficiency of a cyclone with helical-roof inlet, *Powder Technology*, 305, 48-55.

[11]   Pei, B., Yang, L., Dong, K., Jiang, Y., Du, X. and Wang, B. (2017) The effects of cross-shaped vortex finder on the performance of cyclone separator, *Powder Technology*, 313, 135-144.

[12]   Wasilewski, M. and Brar, L.S. (2017) Optimization of the geometry of cyclone separators in clinker burning process: A case study, *Powder Technology*, 313, 293-302.

[13]   Hoekstra, A.J., Derksen, J.J. and van der Akker, H.E.A. (1999) An experimental and numerical study of turbulent swirling flow in gas cyclones, *Chemical Engineering Science*, 51, 2055-2065.

[14]   Xiang, R., Park, S.H. and Lee, K.W. (2001) Effects of cone dimension on cyclone performance, *Journal of Aerosol Science*, 32(4), 549-561.

[15]   Lim, K.S., Kim, H.S. and Lee, K.W. (2004) Characteristics of the collection efficiency for a cyclone with different vortex finder shapes, *Journal of Aerosol Science*, 35(6), 743-754.

[16]   Raoufi, A., Shams, M., Farzaneh, M. and Ebrahimi, R. (2008) Numerical simulation and optimization of fluid flow in cyclone vortex finder, *Chemical Engineering and Processing: Process Intensification*, 47(1), 128-137.

[17]   Elsayed, K. and Lacor, C. (2010) Optimization of cyclone separator geometry for minimum pressure drop using mathematical models and CFD simulations, *Chemical Engineering Science*, 65, 6048-6058.

[18]   Elsayed K. and Lacor C. (2011) The effect of cyclone inlet dimensions on the flow pattern and performance, *Applied Mathmathical Modelling*, 35, 1952-1968.

[19]   Elsayed K. and Lacor C. (2011) Modeling, analysis and optimization of aircyclones using artificial neural network, response surface methodology and CFD simulation approaches, *Powder Technology*, 212, 115-133.

[20]   Sun, X., Zhang, Z. and Chen, D.R. (2017) Numerical modeling of miniature cyclone, *Powder Technology*, 320, 325-339.

[21]   Saltzman, B.E. and Hochstrasser, J.M. (1983) Design and performance of miniature cyclone for respirable aerosol sampling, *Environmental Science & Technology*, 17, 418-424.

[22]   Moore, M.E. and Mcfarland, A.R. (1993) Performance modeling single-inlet aerosol sampling cyclone, *Environmental Science & Technology*, 27, 1842-1848.

[23]   Kim, J.C. and Lee, K.W. (1990) Experimental study of particle collection by small cyclones, *Aerosol Science and Technology*, 12, 1003-1015.

[24]   Zhu, Y. and Lee, K.W. (1999) Experimental study on small cyclones operating at high flowrates, *Journal of Aerosol Science*, 30, 1303-1315.

[25]   Karadeniz, A. (2015) Effect of modifications on stairmand high efficiency type cyclone geometry on particle collection efficiency and pressure drop. *MSc thesis, Yıldız Technical University, Graduate School of Natural and Applied Sciences*, Istanbul, Turkey.

[26]   Demir, S. (2014) A practical model for estimating cyclone pressure drop in cyclone separators: An experimental study, *Powder Technology*, 268, 329-338.

[27]   Muschelknautz, E. (1972) Die berechnung von zyklonabscheidern für gase, *Chemie Ingenieur Technik*, 44, 63-71.

[28]   Cortes, C. and Gil, A. (2007) Modeling the gas and particle flow inside cyclone separators, *Progress in Energy and Combustion Science*, 33, 409-452.

[29]   Chen, J. and Shi, M. (2007) A universal model to calculate cyclone pressure drop, *Powder Technology*, 171, 184-191.